Iranian Journal of Chemical Engineering
Vol. 3, No. 1 (Winter), 2006, IAChE

A Sequential Formulation for Compositional Reservoir Simulation Using Peng Robinson Equation of State

A. Shahrabadi[*]*, B. Dabir*
Chemical Engineering Department, AmirKabir University of Technology, Tehran, Iran.

Abstract

In this paper, a simplified formulation for a compositional reservoir simulator is presented. These type of simulators are used when interphase mass transfer depends on phase composition as well as pressure. The procedure for solving compositional model equations is completely described. The Peng Robinson equation of state is used for preparing a compositional thermodynamic program for equilibrium calculation, property estimation and pseudo component determination. Another purpose of this paper is to prepare an experimental apparatus for the displacement of oil by gas injection. In each test, oil recovery as a function of injected pore volume was measured. The application of the developed simulator to simulate the results of the oil recovery from slim tube experiments is also presented. Finally, the model was run for a 2-D reservoir. Acceptable trends were obtained from the model predictions.

Keywords: *Compositional, Reservoir simulator, Slim tube, Equation of state, Peng Robinson*

Introduction

Numerical reservoir simulation is a vital tool in the petroleum industry. This technique can be used in planning the exploration of new reservoirs, forecasting the behavior of old fields, to make single well studies, and in researching methods to improve hydrocarbon recovery. At the beginning, the numerical models were built by considering three phases in the reservoir (oil, gas and water), but they were unable to treat the compositional variations occurring in each phase. These models are referred to as black oil models. In this case, phase behavior is simply represented by B_o (oil formation volume factor) and R_s(solution gas oil ratio), which are only functions of pressure. Whenever it is inappropriate to use a black oil model, the oil and gas must be described by more than two pseudo-components. In this case, phase behavior is represented by an equation of state and phase equilibrium relations, requiring flash calculations[1]. In this case compositional reservoir simulators must be used. Compositional reservoir simulators are important tools for predicting the performance of oil recovery methods whenever oil and gas undergo vigorous mass transfer during the recovery process. These processes include nitrogen injection into a gas condensate or volatile oil reservoir during the primary production period, and CO_2 or enriched gas injection for enhanced oil recovery. The design of these processes requires an accurate

* - E-mail: a_shahrabadi@yahoo.com

prediction of the vapor liquid equilibrium between oil and gas. Generally this is done by using an equation of state. Recently cubic equations of state such as Peng Robinson and Soave Redlich Kwong appear to be more popular for the correlation of fluid properties.
For compositional simulation two basic solution methods have been proposed. These methods are the "Newton-Raphson" and "Non Newton-Raphson" methods. In the Newton-Raphson method, the iterative technique specifies how the pressure equation is formed. In the Non Newton-Raphson method, the composition dependence of certain terms is neglected to form the pressure equation. From the formulation point of view, several compositional formulations have been published in the literature. They may be classified as IMPECS (Implicit in Pressure, Explicit in Composition and Saturation), semi implicit or IMPSEC (Implicit in Pressure and Saturation, Explicit in Composition), sequential type and FIM (Fully Implicit Method) formulation.
The first compositional simulators of general applications were developed by Kazemi et al.[2] and by Fussel and Fussel[3]. Young and Stephenson[4] classified IMPECS type into the Non-Newton and Newton method. The Non-Newton approach was originally proposed by Nelon[5], other versions were later presented by some authors. These methods differ in the manner in which the pressure equation is formed. The model presented by Acs et al.[6] is a Non-Newton Raphson method in which the pressure equation includes the compositional effects. Watts[7], based on the ideas of Acs et al., presented another approach for the sequential implicit method to solve the compositional flow difference equations. An attempt was made to combine the advantages of IMPECS, while retaining some of the stability characteristics of the implicit method. Quandalle and Savary[8] presented another method. For multiphase flow, the grid block equations are reduced to three equations with three primary unknowns, P (pressure), S_o (oil saturation) and S_w (water saturation). Having these parameters, the subset of the thermodynamic equation is arbitrarily decoupled and used. Celso[9] presented a different approach that was regarded as a semi implicit method. In his method, the Newton iteration was applied to the compositional flow equations that result after considering, explicitly, in flow terms, one iteration behind. Wang et al.[10] presented a fully implicit compositional simulator for large scale reservoir simulation. Their simulator uses a multi block, domain decomposition approach. Recently, compositional stream line simulators for the assessment of miscible/near miscible gas injecttion performance are widely used. These simulators have significant potential to accommodate the requirement for accurate and reliable production forecasts. These requirements include high resolution descriptions of permeability, heterogeneity, and an appropriate representation of phase behavior, including a sufficient number of components in the equation of state.[11]. Numerous authors have contributed to the development of stream line simulators[12-16]. This Paper describes an iterative sequential compositional formulation. Basically it uses the ideas of Nghiem et al.[17], but in this work the implicit transmiscibilities have been used.

Compositional model equations

The starting point for the compositional formulation is the molar continuity equation for any component *i* and water:

$$\frac{\partial N_i}{\partial t} = \theta_i \quad , \quad i = 1,2,...,n_c \tag{1}$$

$$\frac{\partial N_{n_c+1}}{\partial t} = \theta_{n_c+1} \tag{2}$$

N_i denotes the moles of component *i* per unit

of reservoir volume, and N_{n_c+1} is the moles of water per unit of reservoir volume related to the phase molar densities, saturations and composition as follows:

$$N_i = \phi\left(\xi_o S_o x_i + \xi_g S_g y_i\right) \tag{3}$$

$$N_{n_c+1} = \phi \xi_w S_w \tag{4}$$

$\theta_i\left(\theta_{nc+1}\right)$ is the rate of the accumulation of component *i* (water), equal to the divergence of the flux of component *i* plus the rate of injection or production. Thus:

$$\theta_i = \nabla \cdot \left[\xi_o x_i \frac{kk_{ro}}{\mu_o} \nabla \Phi_o + \xi_g y_i \frac{kk_{rg}}{\mu_g} \nabla \Phi_g \right] + q_i \tag{5}$$

$$\theta_{n_c+1} = \nabla \cdot \left[\xi_w \frac{kk_{rw}}{\mu_w} \nabla \Phi_w \right] + q_w \tag{6}$$

In the above equations:

$$\nabla \Phi_o = \nabla P_o - \gamma_o \nabla h \tag{7}$$

$$\nabla \Phi_g = \nabla P_o + \nabla P_{cog} - \gamma_g \nabla h \tag{8}$$

$$\nabla \Phi_w = \nabla P_o - \nabla P_{cow} - \gamma_w \nabla h \tag{9}$$

$$\gamma_j = C_1 \frac{g}{g_c} \rho_j \quad , \quad j = o, g, w \tag{10}$$

The molar continuity equation for the hydrocarbon system is obtained by summing equation 1 over n_c hydrocarbon components:

$$\frac{\partial N}{\partial t} = \theta \tag{11}$$

In this equation:

$$N = \phi\left(\xi_o S_o + \xi_g S_g\right) \tag{12}$$

$$\theta = \nabla \cdot \left[\xi_o \frac{kk_{ro}}{\mu_o} \nabla \Phi_o + \xi_g \frac{kk_{rg}}{\mu_g} \nabla \Phi_g \right] + q_t \tag{13}$$

$$q_t = \sum_{i=1}^{n_c} q_i \tag{14}$$

Multiplying Equations 1,2 and 11 by grid block volume (V_b) and writing in finite difference form:

$$\frac{V_b}{\Delta t}\left(N_i^{n+1} - N_i^n\right) = \Delta\left(T_o^{n+1} x_i^{n+1}\left(\Delta P_o^{n+1} - \gamma_o^n \Delta h\right)\right) + \Delta\left(T_g^{n+1} y_i^{n+1}\left(\Delta P_o^{n+1} + \Delta P_{cog}^n - \gamma_o^n \Delta h\right)\right) + q_i V_b \tag{15}$$

$$\frac{V_b}{\Delta t}\left(N_w^{n+1} - N_w^n\right) = \Delta T_w^{n+1}\left(\Delta P_o^{n+1} - \Delta P_{cow}^n - \gamma_w^n \Delta h\right) + q_w V_b \tag{16}$$

$$\frac{V_b}{\Delta t}\left(N^{n+1} - N^n\right) = \Delta\left(T_o^{n+1}\left(\Delta P_o^{n+1} - \gamma_o^n \Delta h\right)\right) + \Delta\left(T_g^{n+1}\left(\Delta P_o^{n+1} + \Delta P_{cog}^n - \gamma_o^n \Delta h\right)\right) + q_t V_b \tag{17}$$

In the above equations:

$$T_j = C_2 \frac{kk_{rj}}{\mu_j} \frac{A}{\Delta L_t} \quad , \quad j = o, g, w \tag{18}$$

C_1 and C_2 are conversion constants that depend on the units involved.
It is assumed that gas and oil are in phase equilibrium at the end of each time step. This means that the interphase thermodynamic exchange in the reservoir is rapid compared with fluid flow. The condition for thermodynamic equilibrium is established by the equality of the oil and gas phase chemical potential or fugacity for each component:

$$f_i^o(T,P,x_i) = f_i^g(T,P,y_i) \tag{19}$$

From a material balance on oil and gas phases, the following equation is obtained:

$$Fz_i = Lx_i + Vy_i \quad , \quad i = 1,2,...,n_c \tag{20}$$

The following equations are used for solving equation 19:

$$\sum_{i=1}^{n_c} x_i - 1 = 0 \tag{21}$$

$$\sum_{i=1}^{n_c} y_i - 1 = 0 \tag{22}$$

$$\sum_{i=1}^{n_c} \frac{z_i(K_i - 1)}{1 + V(K_i - 1)} = 0 \tag{23}$$

The definition of saturation gives the constraint equation:

$$S_o + S_g + S_w = 1 \tag{24}$$

Each grid block has its own set of the above equations. The basic idea used in this work is to reduce the number of unknowns into one unknown for each grid block in terms of grid block pressure.

Construction of pressure equation
Adding equations 16 and 17 results in the pressure equation:

$$\frac{V_b}{\Delta t}\left[(N+N_w)^{n+1} - (N+N_w)^n\right] = \Delta\left(T_o^{n+1}\left(\Delta P_o^{n+1} - \gamma_o^n \Delta h\right)\right) + \Delta\left(T_g^{n+1}\left(\Delta P_o^{n+1} + \Delta P_{cog}^n - \gamma_g^n \Delta h\right)\right) + \Delta\left(T_w^{n+1}\left(\Delta P_o^{n+1} + \Delta P_{cog}^n - \gamma_w^n \Delta h\right)\right) + V_b\left(q_t + q_w\right) \tag{25}$$

The following approximations apply to the flow terms:

$$T_j^{n+1} = T_j^l \quad , \quad j = o,g,w \tag{26}$$

$$x_i^{n+1} = x_i^l \tag{27}$$

$$y_i^{n+1} = y_i^l \tag{28}$$

l denotes the last iteration. The pressure equation is solved by using the iterative bi-conjugate gradient method for sparse matrices[18].

Composition and saturation equations
The mole fraction of each component is calculated at each iteration by using the pressure of the same iteration. First the number of moles of component i is calculated from equation 15 and then total moles will be obtained from equation 17, and z_i obtained by the ratio of N_i to N:

$$N_i^{l+1} = \frac{\Delta t}{V_b}\left[\Delta\left(T_o^{n+1} x_i^{n+1}\left(\Delta P_o^{n+1} - \gamma_o^n \Delta h\right)\right) + \Delta\left(T_g^{n+1} y_i^{n+1}\left(\Delta P_o^{n+1} + \Delta P_{cog}^n - \gamma_g^n \Delta h\right)\right) + q_i V_b\right] + N_i^n \tag{29a}$$

$$N^{l+1} = \frac{\Delta t}{V_b}\left[\Delta\left(T_o^{n+1}\left(\Delta P_o^{n+1} - \gamma_o^n \Delta h\right)\right) + \Delta\left(T_g^{n+1}\left(\Delta P_o^{n+1} + \Delta P_{cog}^n - \gamma_g^n \Delta h\right)\right) + q_t V\right] + N^n \quad (29b)$$

$$z_i^{l+1} = \frac{N_i^{l+1}}{N^{l+1}} \quad (29c)$$

water saturation is obtained from equation 16:

$$N_w^{l+1} = \frac{\Delta t}{V_b}\left[\begin{matrix}\Delta T_w^{n+1}\left(\Delta P_o^{n+1} - \Delta P_{cow}^n - \gamma_w^n \Delta h\right) \\ + q_w V_b\end{matrix}\right] + N_w^n \quad (30)$$

$$S_w^{l+1} = \frac{N_w^{l+1}}{\left(\phi \xi_o\right)^{l+1}} \quad (31)$$

After calculating compositions, flash calculation is performed on calculated compositions in each grid block at block pressure and temperature to obtain L and V. Then, gas and oil saturations are calculated as:

$$S_g^{l+1} = \frac{V\ \xi_o^{l+1}\left(1 - S_w^{l+1}\right)}{\xi_g^{l+1} + V\left(\xi_o + \xi_g\right)^{l+1}} \quad (32)$$

$$S_o^{l+1} = 1 - S_g^{l+1} - S_o^{l+1} \quad (33)$$

Where:

$$V = \frac{\xi_g S_g}{\xi_o S_o + \xi_g S_g} \quad (34)$$

Solution Procedure

The following procedure to solve the above equations over a time step must be used.

1- Solving the pressure equation (equation 25) by using the iterative bi-conjugate gradient method for sparse matrix[18].
2- Obtaining water saturation (equation 31) and composition of each component (equa-tion 29) in each grid block using the block pressures computed in Step 1.
3- Performing flash calculation on calculated composition in Step 2 at block temperature and pressure in each grid block to obtain L and V.
4- Calculating oil and gas saturations (equations 32, 33).
5- Updating T_j, x_i, y_i, N and N_w..

The above steps are repeated until convergence is achieved.

Results

a- Slim tube simulation (one dimensional case)

The recovery curves obtained in this study were determined by using the slim tube apparatus. The specifications of the apparatus are given in Table 1.

Table 1. Specifications of slim tube

Initial Diameter (mm)	4.65
Length (m)	12.78
Pore Volume (cm^3)	94.73
Porosity (%)	43.7
Permeability (Darcy)	4.850
Porous Media	Glass beads

The tube was initially saturated with reservoir oil. Oil was displaced by gas at a constant injection rate of 15 cm^3/sec. The oil sample used in this work was obtained from an Iranian oil reservoir. Also, a gas sample from a gas reservoir of Iran was used as the displacing agent. The compositional analysis of oil and gas, as well as the characteristics of the plus fraction are given in Tables 2 and 3. Bubble point pressure and swelling data are

also included. About a 1.2 pore volume of gas was injected in each test. At the end of each step produced, the volume of oil and gas were measured. The recovery factor was calculated from the measured volumes of the produced oil and gas. This study is performed to determine the effect of interfacial tension (IFT) on simulating results in slim tube experiments. Five displacement tests at different pressures were performed and the oil recovery as a function of the injected pore volume was recorded. The influence of interfacial tension on the results of the developed model was examined in two simulation runs with different relative permeability curves. The first simulation was performed with fixed relative permeability curves (immiscible condition), while the variable relative permeability curves as a function of both saturation and interfacial tension were used (miscible condition), in the second run. To include interfacial tension (σ) in relative permeabilities, the following curves were used[17].

Table 2. Compositional analysis of oil, gas sample, swelling and saturation data

Components	Reservoir Fluid	Injection Gas	Recombined Reservoir Fluid + Gas					
H2S	0.0012	0.0047	0.001528	0.001873	0.002153	0.002383	0.002571	0.002732
N2	0.0004	0.0414	0.004233	0.008267	0.011532	0.014214	0.016411	0.01829
CO2	0.0125	0.0217	0.013357	0.01426	0.014991	0.015592	0.016084	0.016505
C1	0.2530	0.8490	0.308699	0.367335	0.414793	0.453791	0.485726	0.513042
C2	0.0570	0.0516	0.056494	0.055967	0.055541	0.05519	0.054903	0.054658
C3	0.0471	0.0174	0.044314	0.041388	0.039019	0.037073	0.035479	0.034116
IC4+ NC4	0.0440	0.0086	0.040683	0.037198	0.034377	0.032059	0.030161	0.028538
IC5+ NC5	0.0217	0.0030	0.019949	0.018108	0.016619	0.015394	0.014392	0.013535
C6	0.0398	0.0013	0.036201	0.032417	0.029355	0.026839	0.024778	0.023016
C7	0.0351	0.0010	0.031911	0.02856	0.025847	0.023618	0.021793	0.020232
C8	0.0330	0.0003	0.029941	0.026725	0.024122	0.021983	0.020232	0.018734
C9+	0.4553	0.0000	0.41269	0.367901	0.331651	0.301862	0.277469	0.256604
Solution GOR,M^3/M^3 (Scf/STB)	82 (459.2)	-	94 (529.7)	111 (621.5)	127 (714.0)	144 (806.6)	160 (897.2)	176 (988.4)
Bubble Point Pressure kPa (psia)	11,925 (1730)		14,592 (2117)	17,866 (2592)	21,719 (3151)	24,091 (3495)	26,413 (3832)	29,171 (4232)
Calculated Data								
Bubble Point Pressure kPa (psia)	11,911 (1728)		14,685 (2130.5)	18,021 (2614.5)	21,126 (3064.9)	24,031 (3486.4)	26,715 (3875.7)	29,287 (4248.9)
Swelling factor	1.00		1.03	1.07	1.11	1.14	1.18	1.21

Table 3. Characteristics of plus fraction

Molecular Weight	194
Specific Gravity	0.8897

$$k_{ro} = \left(1 - e^{-a_o r}\right)\bar{k}_{ro} + e^{-a_g r} S_o \quad (35)$$

$$k_{rg} = \left(1 - e^{-a_g r}\right)\bar{k}_{rg} + e^{-a_g r} S_g \quad (36)$$

In the above equations, $r = \frac{\sigma}{\sigma^*}$ and a_g, a_o are positive numbers and used as adjustable parameters. Interfacial tension between vapor and liquid phases at 20,678 kPa (3000 psia) and 83°C (181°F) at equilibrium was considered as base IFT (σ^*). Generally, in a two phase system, as the IFT between phases decreases, the curvature as well as the residual saturation decreases. In the extreme case of zero IFT, the relative permeability curves become two straight lines and the value of the relative permeability of each phase will be equal to the value of its saturation. The following equations were used for $\bar{k}_{rg}$, $\bar{k}_{ro}$:

$$\bar{k}_{rg} = S_g^2 \quad (37)$$

$$\bar{k}_{ro} = \left(\frac{S_o - 0.2}{0.8}\right)^3 \quad (38)$$

A one dimensional compositional model composed of 30 grid blocks was employed to simulate slim tube experiments. Figures 1 through 5 show the predicted oil recovery versus injected gas volume for the two simulated runs with different relative permeability curves at different pressures. The experimental data are also included in the Figures. Generally, recovery versus pore volume injection is a well-known plot to illustrate, evaluate and compare the results of laboratory flood tests. The produced and injected volumes are the same before breakthrough, and so the resulting curve is a straight-line. Then, it starts to deviate from the straight trajectory. The slope of the curve portion decreases with increasing injected gas volume, finally leveling off. The point where it starts to deviate from the straight line and the level at which it becomes horizontal, is of great importance in making comparisons.

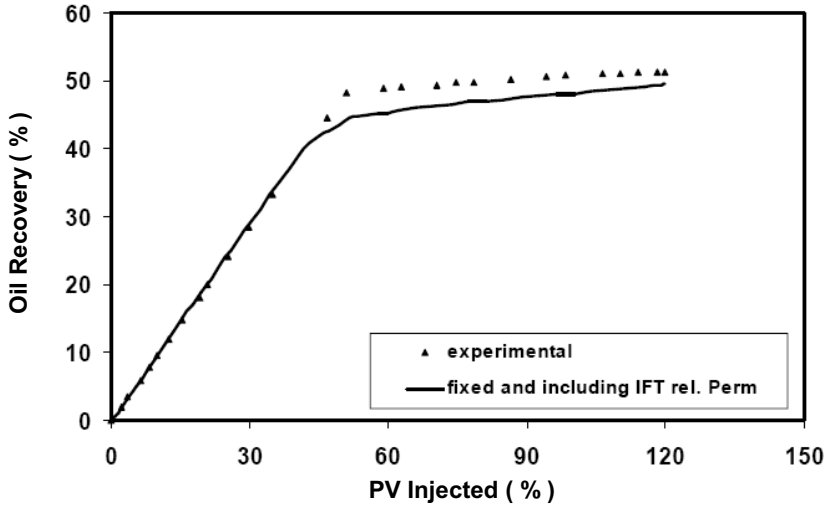

Figure 1. Recovery curve vs. PV injected at pressure 13,786 kPa (2000 psia)

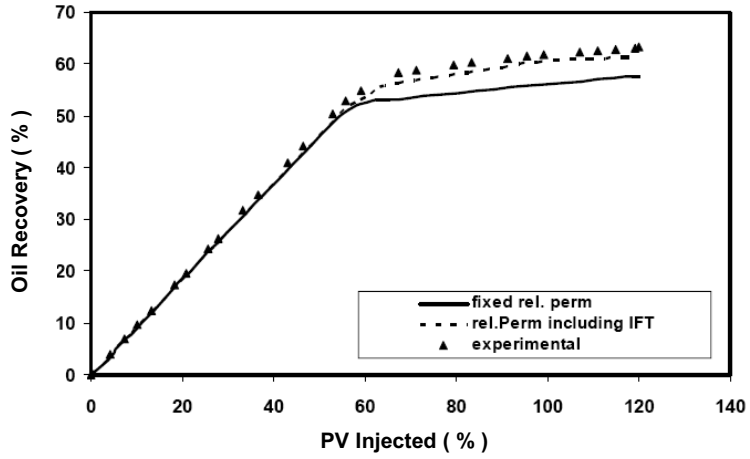

Figure 2. Recovery curve vs. PV injected at pressure 20,678 kPa (3000 psia)

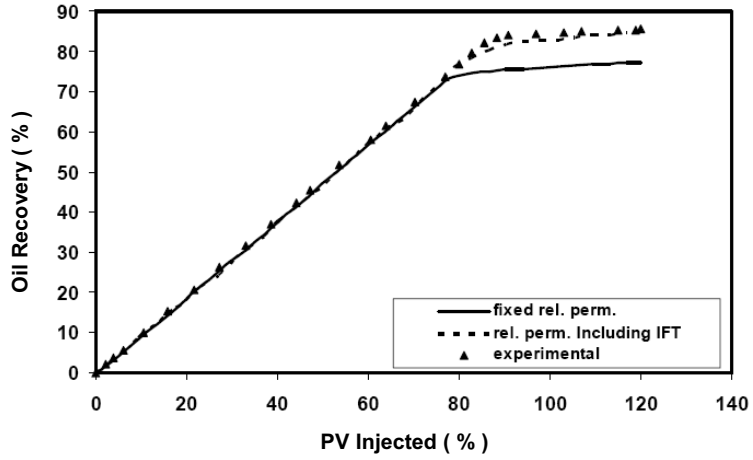

Figure 3. Recovery curve vs. PV injected at pressure 34,464 kPa (5000 psia)

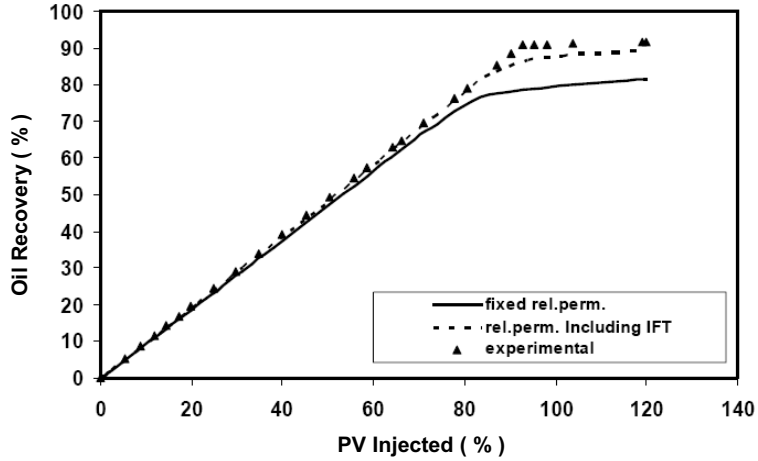

Figure 4. Recovery curve vs. PV injected at pressure 41,357 kPa (6000 psia)

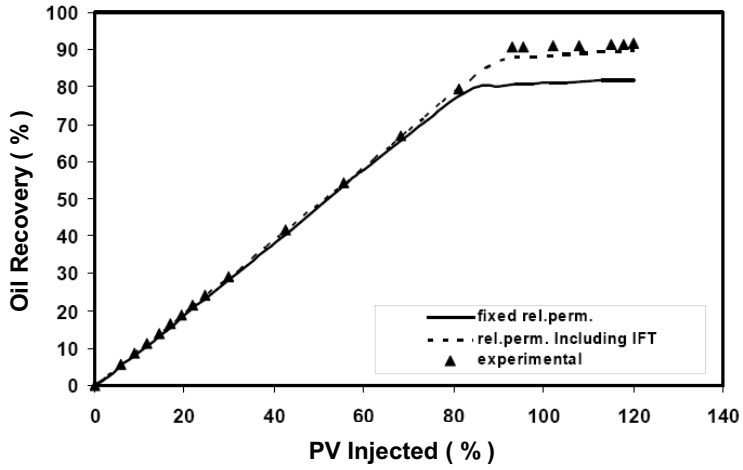

Figure 5. Recovery curve vs. PV injected at pressure 44,804 kPa (6500 psia)

Comparisons show that the results from the run with fixed relative permeability curves underestimate the oil recoveries, while the run with interfacial tension in relative permeabilities improves the predictions. The difference between ultimate oil recoveries obtained using fixed relative permeability and IFT included in curves, is little at low pressure, but significant at high pressures. This is due to the fact that low pressure corresponds to the immiscible zone, and hence IFT has a low effect on the recovery results. Therefore, including IFT in relative permeability curves can not improve the predictions at low pressures, but as pressure increases, the predictions show a good match with the experimental results in a closer margin. In other words, high pressure corresponds to the miscible zone, and so IFT plays a key role in oil recovery. Therefore, including IFT in relative permeability curve improves the results of the model drastically at high pressure regions. The effect of pressure on the recovery can be easily seen while looking at Figure 6, showing performance curves at various pressures. The greater the injection pressure, the higher the ultimate recovery.

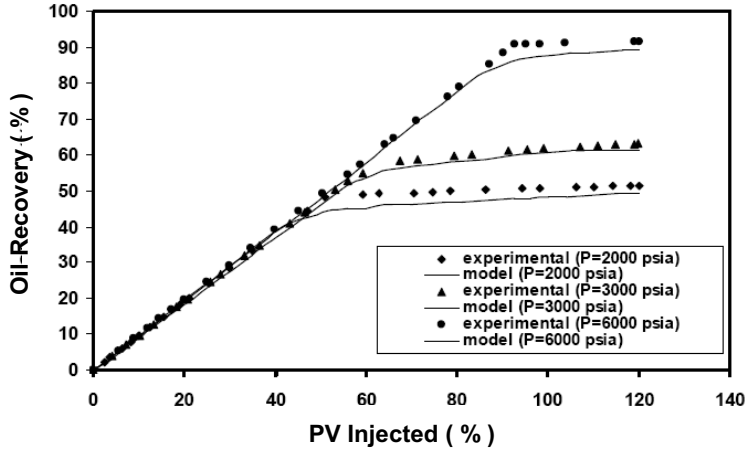

Figure 6. Oil recovery curves at different pressures

b-Areal run (two dimensional case)

The pattern shown in Figure 7 was considered for the gas injection process. This pattern was simulated using an areal 10×10 grid system. Two injectors and two producers were considered. The bottom hole pressure for injectors and producers were 38,600 kPa (5600 psia) and 32,397 kPa (4700 psia) respectively.

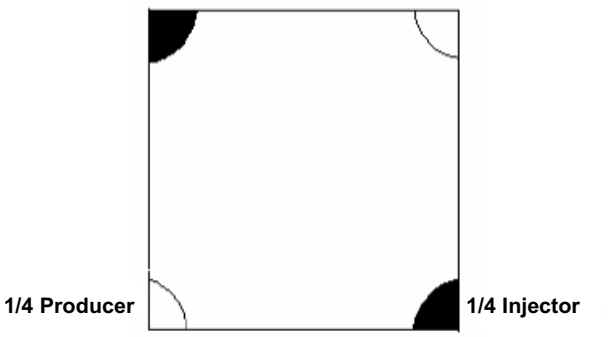

Figure 7. The pattern used in areal run

Additional required data are given in Table 4.

Table 4. Required data for areal run

Length of reservoir,m (ft)	900 (2951)
Width of reservoir, m (ft)	900 (2951)
Thickness, m (ft)	6 (20)
Permeability (mdarcy)	40
Porosity (%)	18
Initial reservoir pressure , kPa (psia)	34,465(5000)
Reservoir temperature , ^{o}C (^{o}F)	83 (181)
Initial water saturation	0.4

Figure 8 shows the gas saturation contours at 1840 days after gas injection. In this figure, no miscible region was found and therefore the process was immiscible.

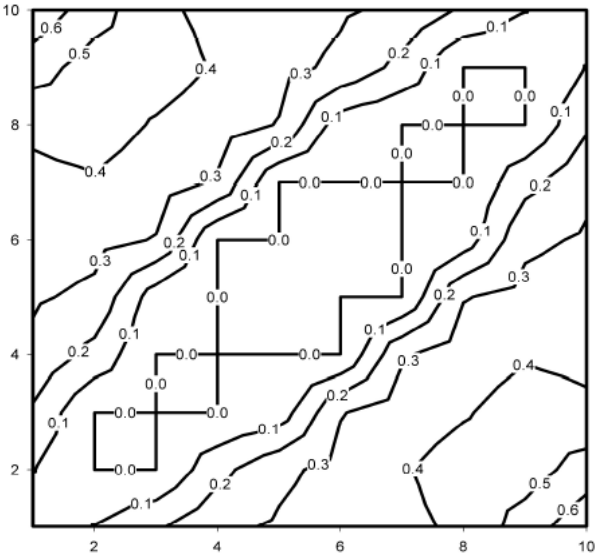

Figure 8. Gas saturation contours at 1840 days after gas injection

The pressure and methane mole fraction distributions of the reservoir are shown in Figures 9 and 10. These curves confirm each other and show good trends compared with anticipated real reservoir behavior. Hence, the application of the developed model for the prediction of reservoir behavior seems to be successful.

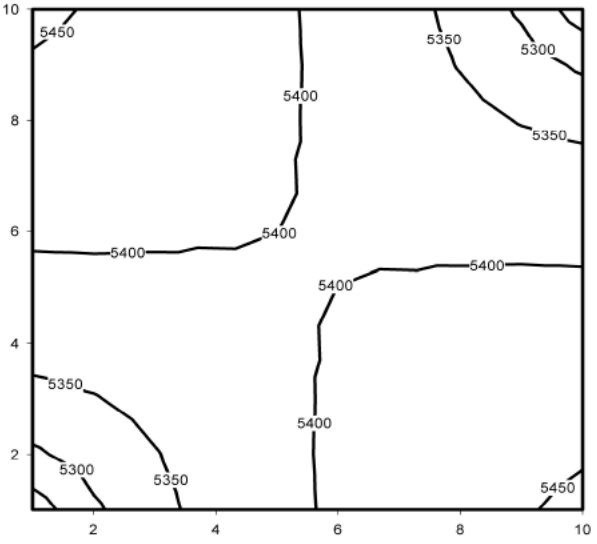

Figure 9. Pressure contours at 1840 days after gas injection

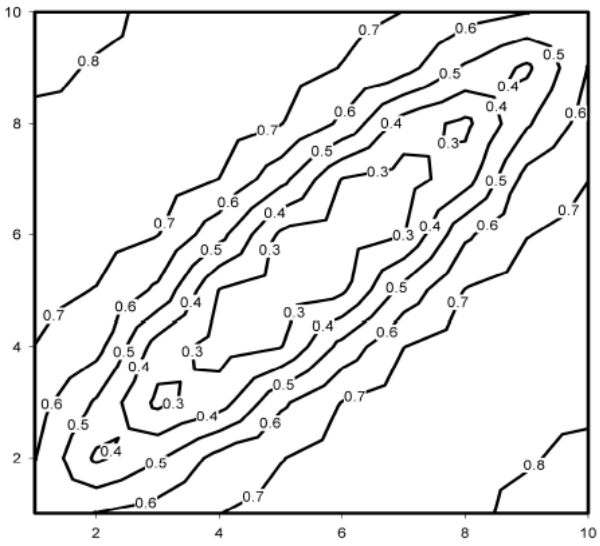

Figure 10. Methane mole fraction contours at 1840 days after gas injection

Conclusion

In this work the formulation procedure of a three phase compositional reservoir model and the method of solving compositional model equations were described. Also, an experimental setup using a slim tube was prepared and some displacement tests were carried out. The oil recovery at different injected volumes was measured during each test. The model predictions were then compared against measured laboratory re-covery data. The effect of including IFT in relative permeability curves on the outputs from the model was also studied. Com-parison between model outputs with and without, including IFT in relative per-meability curves, indicated that having IFT in relative permeability curves has no effect (rather a minor effect) on model results at low pressures, while it was considerable at high pressures. Acceptable results were obtained from the areal run with respect to the anticipated real reservoir behavior. Consequently, the comparison of the slim tube results with the model predictions and areal run predictions, indicate the possibility of employing this model for the reservoir behavior prediction.

Nomenclature

A	area perpendicular to flow (ft^2)
B_o	oil formation volume factor (bbl/STB)
C_1	conversion factor in equation 10
C_2	conversion factor in equation 18
F	feed
f_i^j	fugacity of component i in phase j (atm)
g	gravitational acceleration (ft/s^2)
h	depth (ft)
k	absolute permeability (mdarcy)
k_{rj}	relative permeability of phase j (immiscible condition)
$\overline{k}_{rj}$	relative permeability of phase j (miscible condition)
K_i	K-value of component i
L	ratio of moles in liquid phase to the total number of moles in the mixture
L_t	length (ft)
N	moles of total hydrocarbon per unit of reservoir volume ($\frac{lb-mole}{ft^3}$)
N_i	moles of component i per unit of reservoir volume ($\frac{lb-mole}{ft^3}$)
N_{n_c+1}	moles of water per unit of reservoir volume ($\frac{lb-mole}{ft^3}$)
P	pressure of mixture at equilibrium ($psia$)
P_j	pressure of phase j (psia)
P_{cog}	oil / gas capillary pressure (psia)
P_{cow}	water / oil capillary pressure (psia)
q_i	molar injection / production rate of component i per unit volume ($\frac{lb-mole}{ft^3.day}$)
q_t	molar injection / production rate of hydrocarbon per unit volume ($\frac{lb-mole}{ft^3.day}$)

q_w molar injection / production rate of water per unit volume ($\frac{lb-mole}{ft^3.day}$)

r ratio of IFT to base IFT

R_s gas oil ratio (SCF/STB)

S_j saturation of phase j

t time (day)

T temperature (^oR)

T_j transmissibility of phase j ($\frac{lb-mole}{psia.day}$)

V ratio of moles in vapor phase to the total number of moles in the mixture

V_b block volume (ft^3)

x_i mole fraction of component *i* in oil phase

y_i mole fraction of component *i* in gas phase

z_i mole fraction of component *i* in hydrocarbon

Greek Symbols

θ_i the rate of accumulation of component *i* ($\frac{lb-mole}{ft^3.day}$)

θ_{n_c+1} the rate of accumulation of water ($\frac{lb-mole}{ft^3.day}$)

θ the rate of accumulation of total hydrocarbon ($\frac{lb-mole}{ft^3.day}$)

ϕ porosity

γ_j specific weight of phase j ($\frac{lb}{ft^3}$)

μ_j viscosity of phase *j* (cP)

ρ_j mass density of phase *j* ($\frac{lb}{ft^3}$)

ξ_j molar density of phase *j* ($\frac{lb-mole}{ft^3}$)

Δ difference operator

∇ gradient operator

$\nabla\cdot$ divergence operator

Φ_j potential of phase *j* (psia)

σ interfacial tension ($\frac{dyne}{cm}$)

σ^* base interfacial tension ($\frac{dyne}{cm}$)

References

1. Cao, H., "Development of Techniques for General Purpose Simulators," Ph.D. Dissertation, Stanford University, June 2002.
2. Kazemi, H., Vestal, C.R., and Shank, G.D., "An Efficient Multicomponent Numerical Simulator," Soc. Pet. Eng. J., 355 (Oct. 1978).
3. Fussell, L. T., and Fussell, D. D., "An Iterative Technique for Compositioml Reservoir Models," Soc. Pet. Eng. J., 211(Aug. 1979).
4. Young, L. C., and Stephenson, R. E., "A Generalized Compositional Approach for Reservoir Simulation," Soc. Pet. Eng. J., 728 (Oct. 1983).
5. Nelon, J. S., "Numerical Simulation of Compositional Phenomena in Petroleum Reservoir," paper SPE 4274 presented at 3rd SPE Symposium on Reservoir Simulation, Houston, Texas, (1973).
6. Acs, G., Doleschall, S., and Frakas, E., "General Purpose Compositional Model," Paper SPE 10515 presented at 6th SPE Symposium on Reservoir Simulation, New Orleans, (1982).
7. Watts, J.M., "A Compositional Formulation of the Pressure and Saturation Equations," Paper SPE 12244 presented at 7th SPE Symposium on Reservoir Simulation, San Francisco, (1983).
8. Quandalle, P., and Savary, D., "An Implicit in Pressure and Saturations Approach to Fully Compositional Simulation," paper SPE 18423 presented at Symposium on Reservoir Simulation, Houston,Texas, (1982).
9. Celso Branco, M., and Rodriguez, F., "A Semi Implicit Formulation for Compositional Reservoir Simulation," SPE Advanced Technology Series, 4(1), 171(1995).
10. Wang, P., Balay, S., Sepehrnoori, K., Wheeler, J., Abate, J., Smith, B., and Pope, G.A., "A Fully Implicit Parallel EOS

Compositional Simulator for Large Scale Reservoir Simulation," paper SPE 51885 presented at the 15th Symposium on Reservoir Simulation. Houston, Texas, (1997).
11. Jessen, K., and Orr Jr., F.M., "Gravity Segregation and Compositional Reservoir Simulation," paper SPE 89448 presented at the 14th symposium on improved oil recovery, Tulsa, Oklahoma, (2004).
12. Datta-Gupta, A., and King, M.J., "A Semi Analytical Approach to Tracer Flow Modeling in Heterogeneous Permeable Media," Advances in Water Resources , 18, 9 (1995).
13. Thiele, M.R., Batycky R.P., Blunt, M.J., and Orr Jr., F.M., "Simulating Flow in Heterogeneous Media Using Streamtubes and Streamlines," SPE Reservoir Engineering, 10(1), 5 (1996).
14. Crane, M., Bratvedt, F., Bratvedt, K., and Olufsen, R., "A Fully Compositional Streamline Simulator," paper SPE 63156 presented at the SPE Annual Technical Conference and Exhibition, Dallas, Texas, (2000).
15. Ichiro, O., Datta-Gupta, A., and King, M.J., "Time Step Selection During Streamline Simulation Via Transverse Flux Correction," paper SPE 79688 presented at the SPE Reservoir Simulation Symposium, Houston, Texas, (2003).
16. Seto, C.J., Jessen, K., and Orr Jr., F.M., "Compositional Streamline Simulation of Field Scale Condensate Vaporization by Gas Injection," paper SPE 79690 presented at the SPE Reservoir Simulation Symposium, Houston, Texas, (2003).
17. Nghiem, L.X., Fong, D.K., and Aziz, K., "Compositional Modeling with an Equation of State," Soc. Pet. Eng. J., 687(Dec. 1981)
18. Press, W.H., Teukolsky, S.A., Vetterling, W.T., and Flannery, B.P., "Numerical Recipes in Fortran 77," Cambridge University Press 1992.